Electronic Supporting Information

A Scalable and Biomimetic Approach for TiO_2 Deposition: Enabling Water Splitting by Nanostructured WO_3 in Neutral Media as an Example

Yi-Hsuan Lai,[*a,b] Yu-Ju Lai [b], Chen-Yang Yen [a,b], and Ping-Chang Chuang [b]

[a] Department of Materials Science and Engineering, National Cheng Kung University, No.1, University Road, Tainan City 701, Taiwan.

[b] Department of Materials and Optoelectronic Science, National Sun Yat-sen University 70 Lienhai Rd., Kaohsiung 80424, Taiwan

* Corresponding author: yhlai@gs.ncku.edu.tw

Contents

Experimental	page S2-S3
Supporting Figures S1–S15	page S4-S15
References	page S11

Experimental

Preparation of nanoWO_3 and nanoWO_3|LbL-TiO_2: NanoWO_3 photoanode was prepared by the hydrothermal method as reported.[1] To prepare nanoWO_3|LbL-TiO_2, positively charged protamine sulfate was firstly adsorbed on nanoWO_3 by immersing the nanoWO_3 electrode into a pH 8.5 tris(hydroxymethyl) aminomethane (TRIS) buffer solution (20 mM, 99.9%, Sigma-Aldrich) containing protamine sulfate (2.5 mg mL^{-1}, Sigma-Aldrich) for one h. After rinsing with tris(hydroxymethyl) aminomethane buffered solution, the positively charged nanoWO_3 was immersed in 50 mM titanium(IV) bis(ammonium lactato)dihydroxide (TALH, 50wt% in H_2O, Sigma-Aldrich) solution or 30 minutes to adsorb the negatively charged TALH. The excess TALH was removed by rinsing with the TRIS buffered solution. The procedures were cyclically applied to absorb protamine sulfate and TALH until the desired layers were conducted. After drying at room temperature, the electrode was heated to 500^oC under air for one h with a ramping rate of 5 ^oC min^{-1}.

Preparation of catalysts modified photoanodes: The electrodes, nanoWO_3 or nanoWO_3|LbL-TiO_2, were immersed in a $FeCl_3 \cdot 6H_2O$ solution (5 mM) for 30 min at room temperature, followed by rinsing with water and dried at 60°C. [2] Before the deposition of CoO_x-P_i, the FeOOH modified electrodes were subjected to an electrochemical treatment in a P_i solution (0.5 M, pH 7), in which the potential was held at -1.0 V vs Ag/AgCl/ KCl_{sat} for 10 s followed by at 0.678 V vs Ag/AgCl/ KCl_{sat} for another 10s. The process was repeated for six cycles. Subsequently, CoO_x-P_i was deposited onto the photoanode by photo-deposition from a 0.1 M P_i buffer containing 0.5 mM $Co(NO_3)_2 \cdot 6H_2O$ at pH 7. A potential was held at 0.75 V vs RHE for 20 min.

Materials Characterization: The surface morphologies of the electrodes were characterised by using a Field-Emission scanning electron microscope (SEM, JEOL-6330). The grazing incident X-ray diffraction (GI-XRD) analyses were carried out using a multi-function high power X-Ray diffractometer (Bruker D8). A transmission electron microscope (TEM, JEOL JEM-3010) was used to record the bright field microscopy and selected area diffraction (SAED) images, whereas the equipped Energy-dispersive X-ray spectroscopy (OXFORD INCA x-stream) is used to analyse the

elemental compositions of nanoWO_3|LbL-TiO_2. TEM samples were prepared by Triplebeam FIB-SEM system (Hitachi NX2000), and a carbon layer was deposited onto the samples by 108C Auto Carbon Coater before being sliced focused ion beam (FIB). Surface compositions and chemical states of the electrode were analysed by X-ray photoelectron spectroscopy (XPS, JEOL JPS-9010) using a high power monochromatic Mg Kα radiation (1486.6 eV, 400 μm spot size, 36 W). All peaks are calibrated by using C element to 285 eV.

To find the isoelectric point of WO_3, WO_3 was scratched from the FTO substrate and then suspended in water with different pH, in which pH was adjusted by HCl. On the other hand, to track the zeta potential of WO_3, nanoWO_3 coated with protamine, and nanoWO_3 coated with protamine followed by coated with TALH in a pH 8.5 solution, samples were suspended in TRIS buffer solution (20 mM). The samples suspended in solution was subjected to measurements by a Malvern Zetasizer (Nano ZS90). Data were averaged over three measurement runs, and data evaluation was performed using the Smoluchowski Approximation and General Mode Analysis (Malvern Zetasizer Software v6.20).

PEC measurements: The PEC measurements were recorded with a CHI (mode 7273E) using a two-compartment electrochemical cell. The cell is separated with a proton exchange membrane (Nafion 117^{TM}). The working electrode and an Ag/AgCl/KCl_{sat} reference electrode were placed in the same compartment, whereas a Pt foil, the counter electrode, was placed in another compartment. The potentials were converted to RHE by using E (V vs. RHE) = E (V vs. Ag/AgCl/KCl_{sat}) + 0.197 + 0.059 ×pH unless otherwise noted. For PEC analyses, the geometric working areas of approximate 0.5 cm^2 of the photoelectrodes were defined using a polyester tape. The precise geometric area was determined after the analyses. A solar light simulator (SAN-ElECTRIC, XES-40S2-CE, AAA class) equipped with air mass 1.5 global (AM 1.5G) filter was used as the light source. The illumination intensity was calibrated to 100 mW cm^{-2} by a monocrystalline silicon solar cell. For visible light irradiation, a 420 nm cut-off filter was additionally equipped.

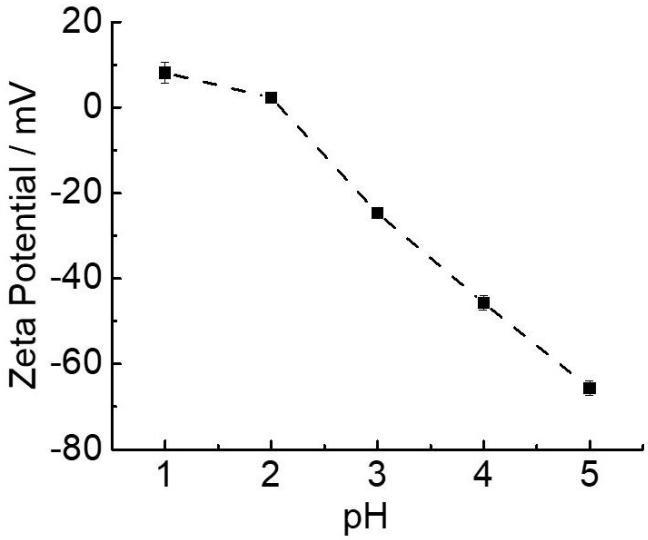

Fig. S1 Zeta potential of nanoWO_3 in aqueous HCl solutions with various pH. The isoelectric point of nanoWO_3 is approximate at pH 2.

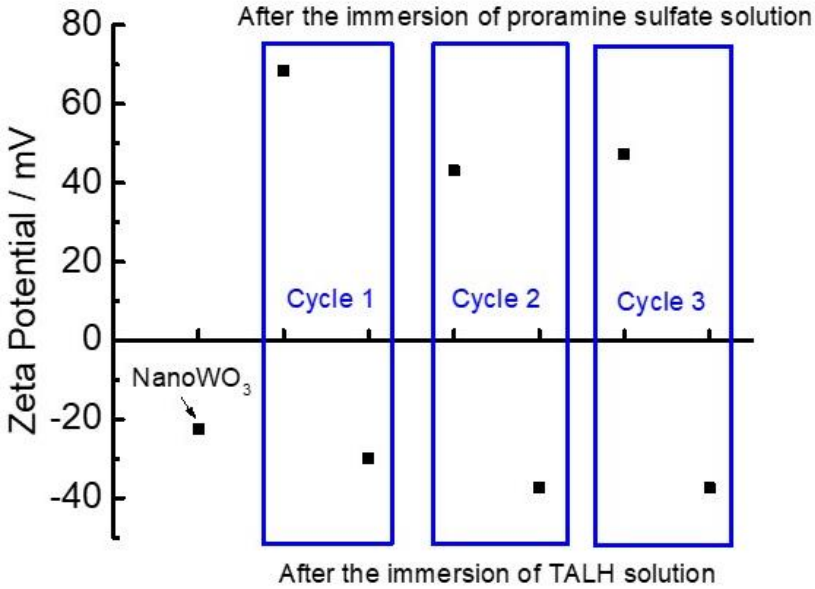

Fig. S2 Zeta potential of nanoWO_3 and protamine-induced LbL deposition on nanoWO_3 with cycles 1 to 3. All samples were measured in TRIS buffered solution (pH 8.5).

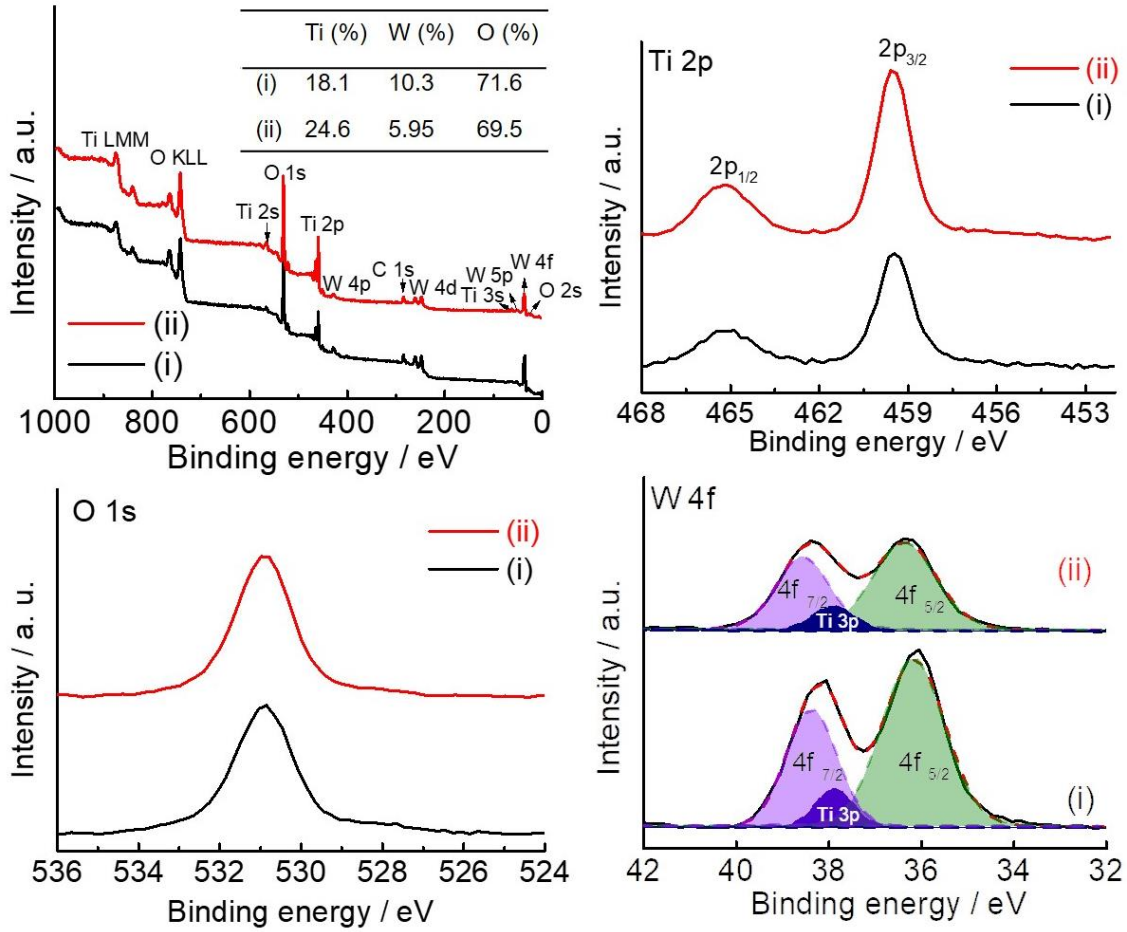

Fig. S3 XPS spectra of (i) nanoWO$_3$|LbLTiO$_2$ (N=1) and (ii) nanoWO$_3$|LbLTiO$_2$ (N=3). The inset in the wide scan shows the atomic percentage of Ti, W, and O. In the Ti region, two peaks centre at 465.9 eV ($2p_{1/2}$) and 459.5 eV ($2p_{3/2}$) core levels confirm the presence of TiO$_2$ on nanoWO$_3$|LbLTiO$_2$.[3] In the core regions of W 4f, Ti 3p is overlapped with W 4f $_{7/2}$ and W 4f $_{5/4}$[4] and Ti 3p is deconvoluted from W 4f for the calculation of the atomic percentage of W.

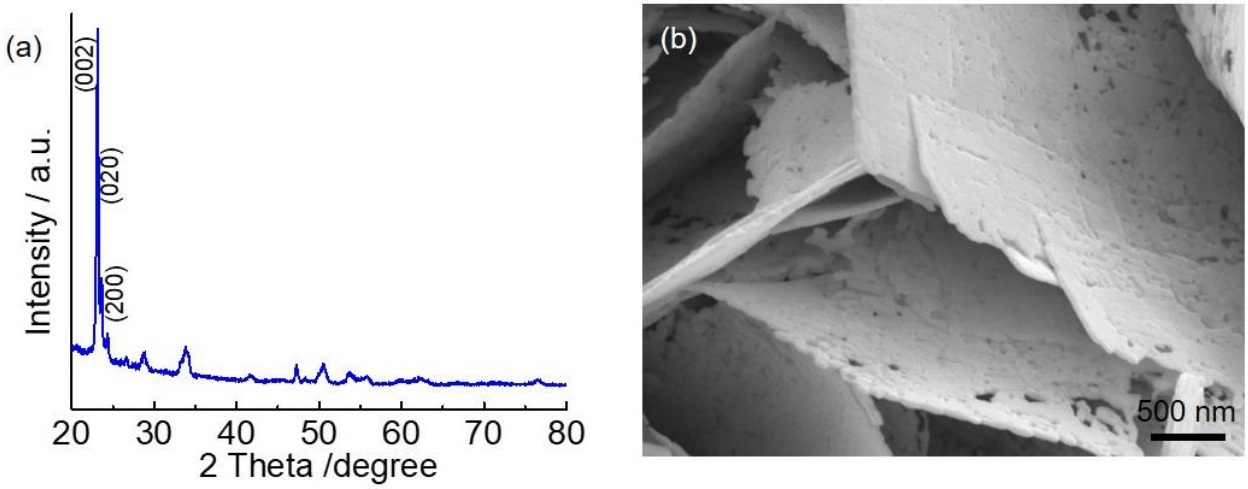

Fig. S4 (a) XRD pattern and (b) SEM image of nanoWO$_3$. The XRD pattern confirms a monoclinic phase for nano WO$_3$ (JCPDS 43-1035).

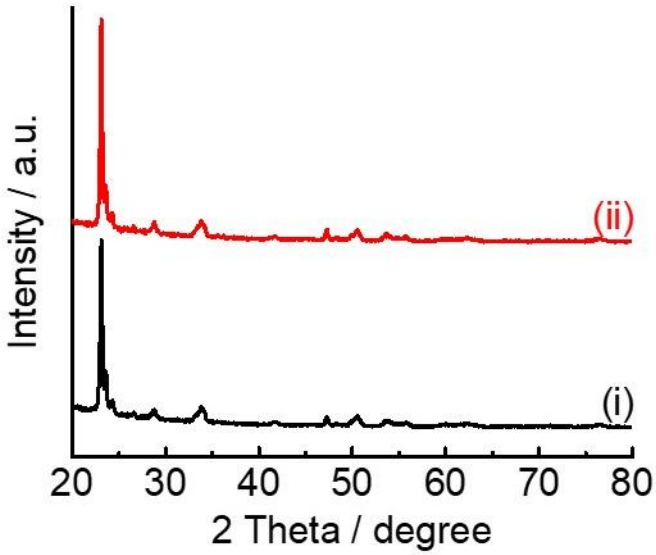

Fig. S5 XRD patterns of (i) nanoWO$_3$ and (ii) nanoWO$_3$|LbLTiO$_2$ (N=1).

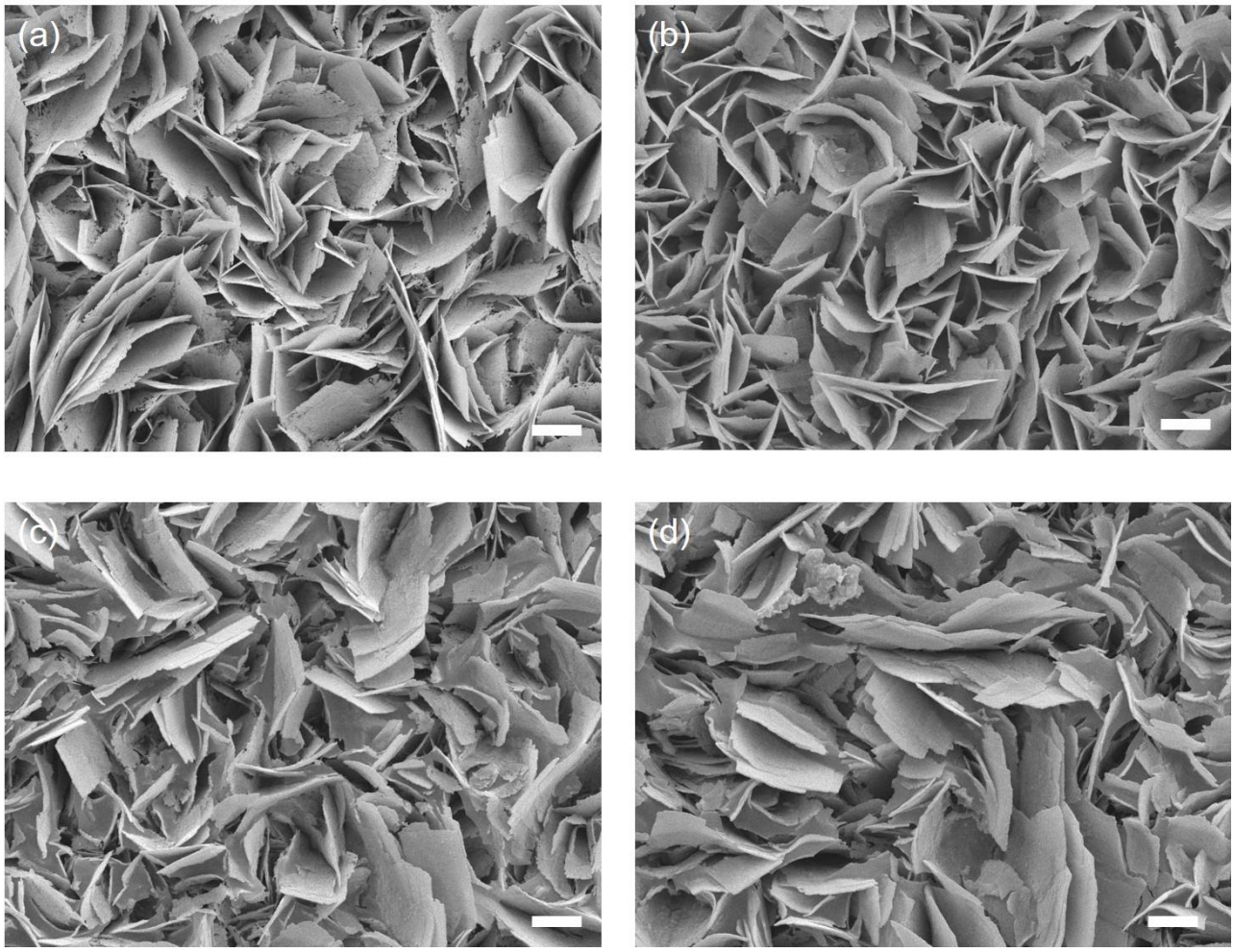

Fig. S6 SEM images of (a) nanoWO$_3$, (b) nanoWO$_3$|LbLTiO$_2$ (N=1), (c) nanoWO$_3$|LbLTiO$_2$ (N=2), and (d) nanoWO$_3$|LbLTiO$_2$ (N=3). Scale bar: 2 μm.

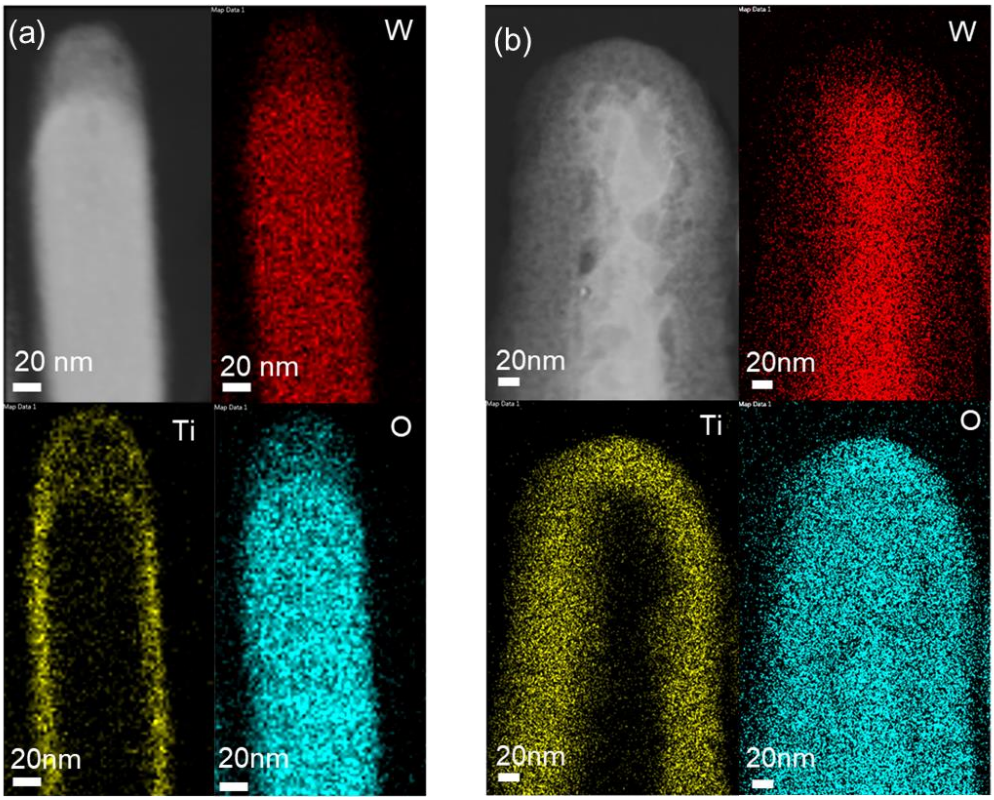

Fig. S7 TEM image and the corresponding elemental mapping images of (a) nanoWO$_3$|LbLTiO$_2$ (N=1) and (b) nanoWO$_3$|LbLTiO$_2$ (N=3). It should be noticed that the samples were being tilted for efficient signal collection, and the scale bars are not corrected with the tilt angle.

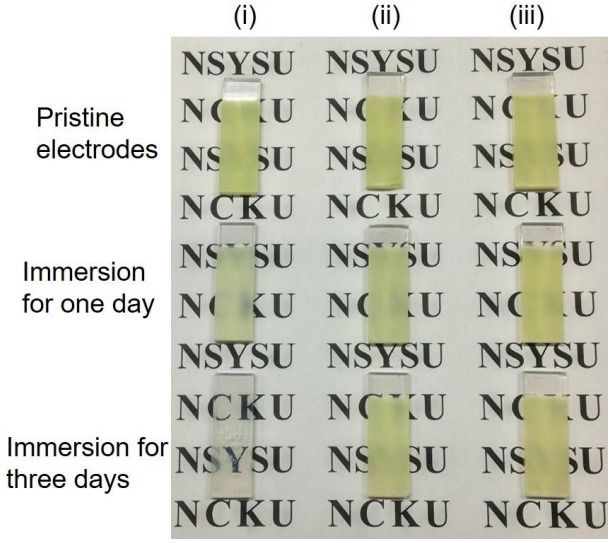

Fig. S8 The digital picture of (i) nanoWO$_3$, (ii) nanoWO$_3$|LbLTiO$_2$ (N=1), and (iii) nanoWO$_3$|LbLTiO$_2$ (N=3) before, after one day, and three days immersion in a neutral P_i solution (0.5 M, pH 7).

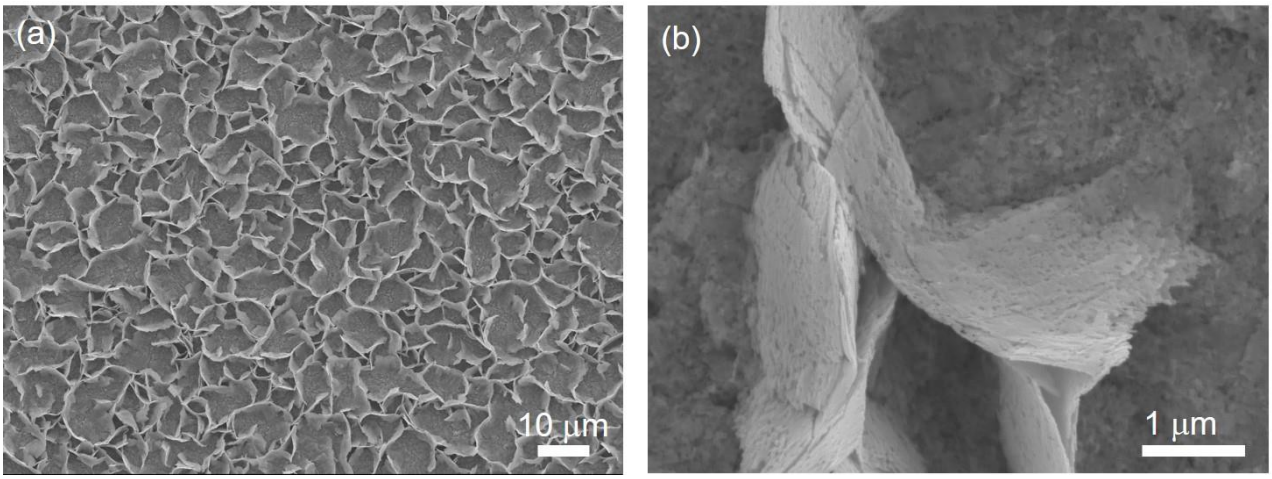

Fig. S9 The SEM images of nanoWO_3, which was annealed at 500 ^oC again after one day of immersion in 0.5 M P_i buffer (pH 7).

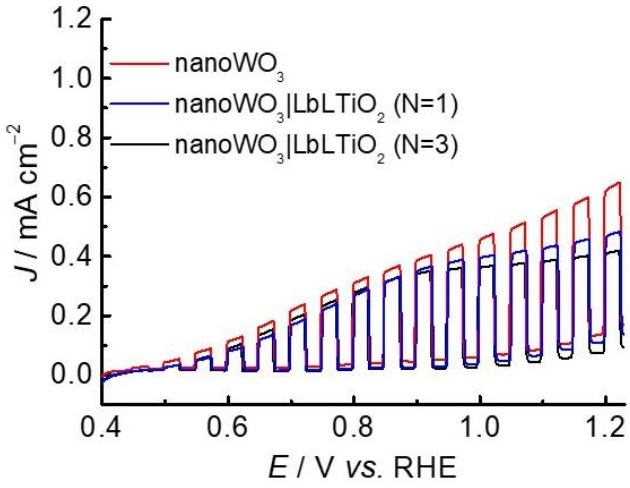

Fig. S10 *J-E* characteristics of photoelectrodes under chopped visible light irradiation (with a 420 nm cut-off filter) in an aqueous 0.5 M P_i buffer solution containing 1 M Na_2SO_3 (pH 7) with a scan rate of 5 mVs^{-1}.

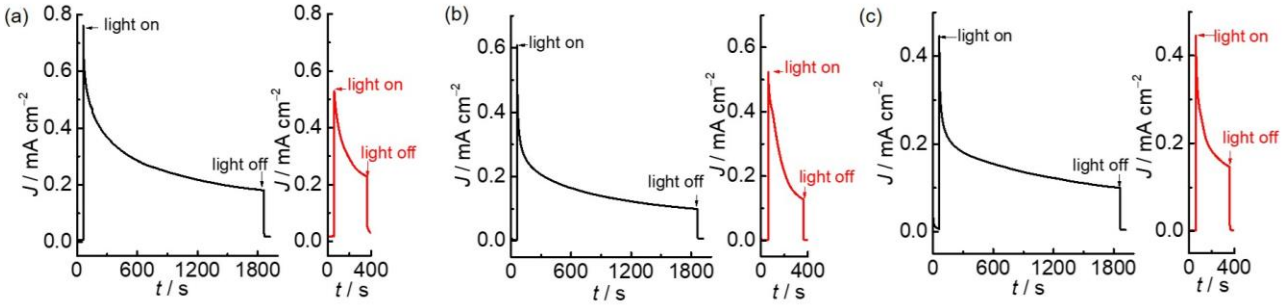

Fig. S11 Chronoamperometry measurements at 1.0 V vs RHE in a 0.5 M P_i buffer (pH 7) of (a) nanoWO_3 (black line) and the same nanoWO_3 after annealing at 500 °C for 1 hour (red line), (b) nanoWO_3|Lb$LTiO_2$ (N=1) (black line) and the same nanoWO_3|Lb$LTiO_2$ (N=1) after annealing at 500 °C for 1 hour (red line), and (c) nanoWO_3|Lb$LTiO_2$ (N=3) (black line) and the same nanoWO_3|Lb$LTiO_2$ (N=3) after annealing at 500 °C for 1 hour (red line).

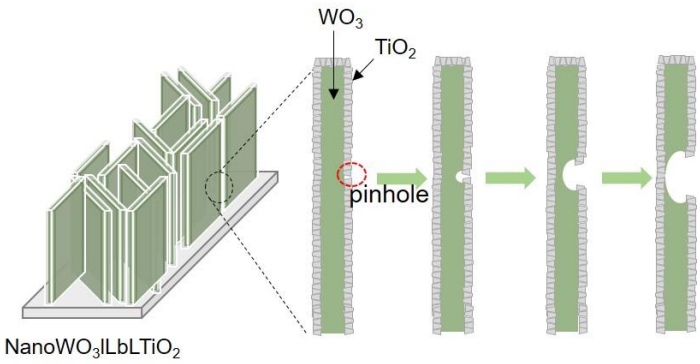

Fig. S12 Schematic representation of the WO_3 corrosion in nanoWO_3|Lb$LTiO_2$ during PEC water oxidation. The formation of soluble tungsten peroxo-species is possibly initiated at the pinhole and expanded through successive dissolution.

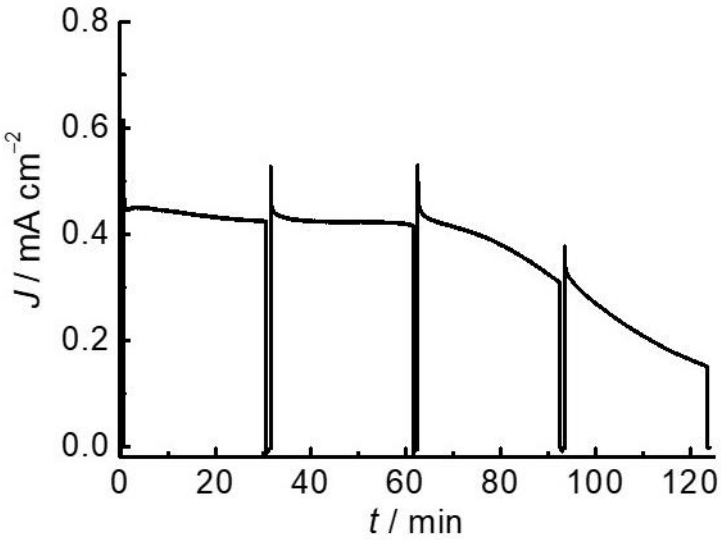

Fig. S13 Chronoamperometry measurement of nanoWO$_3$|LbLTiO$_2$|FeOOH|CoOx-P$_i$ at 1.0 V vs RHE under solar light irradiation (AM 1.5G, 100 mW cm^{-2}). Measurement was recorded in an aqueous 0.5 M P$_i$ buffer (pH 7)

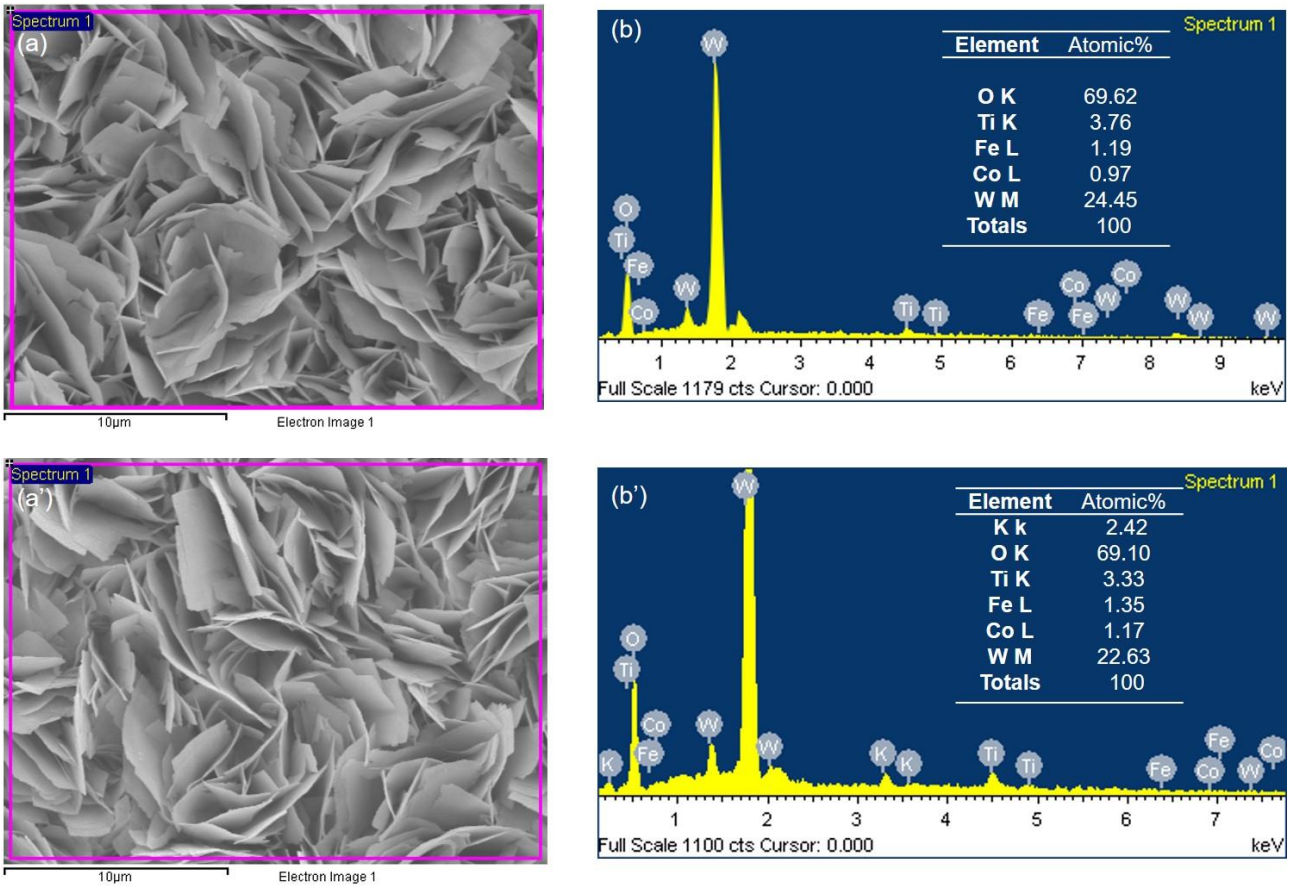

Fig. S14 SEM images and corresponding energy-dispersive X-ray spectroscopy (EDS) results of (a,b) as-prepared nanoWO$_3$|LbLTiO$_2$|FeOOH|CoO$_x$-P$_i$ and (a',b') nanoWO$_3$|LbLTiO$_2$|FeOOH|CoO$_x$-P$_i$ after 3h PEC water oxidation at 1.0 V vs. RHE in a 0.5 M P$_i$ buffer solution. No significant changes on the morphology and compositions are observable for nanoWO$_3$|LbLTiO$_2$|FeOOH|CoO$_x$-P$_i$ after PEC water oxidation, except additional signal of potassium contributed by the electrolyte was detected.

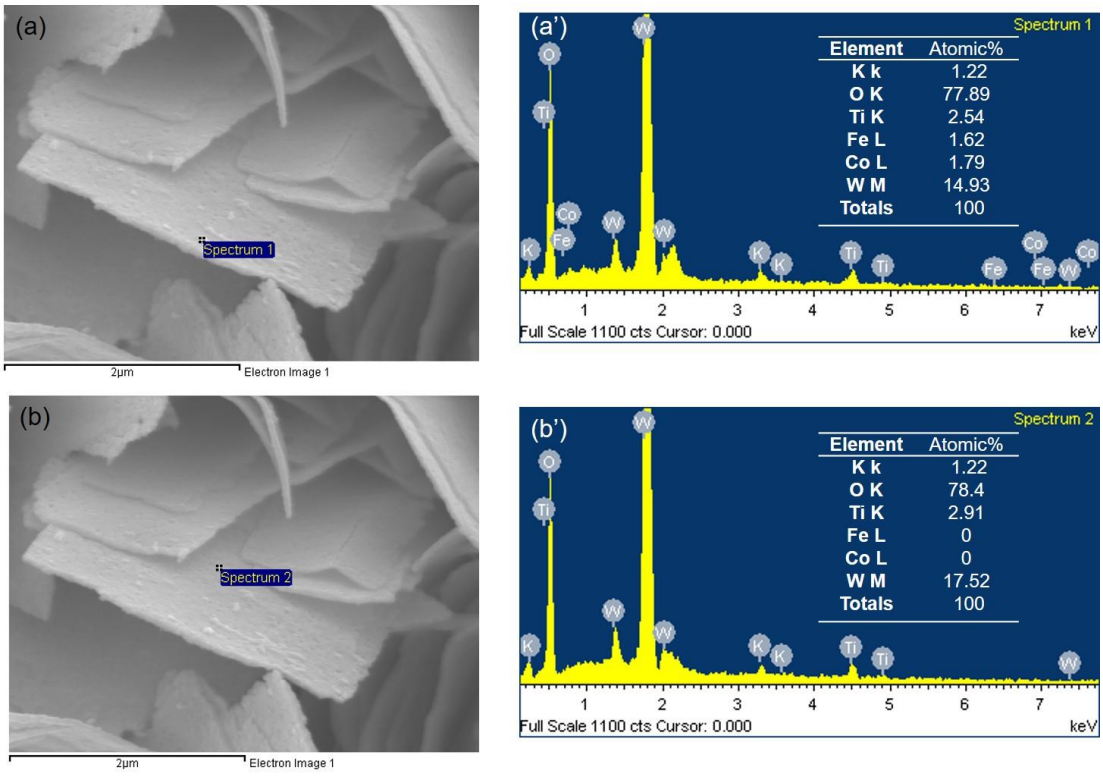

Fig. S15 SEM image and EDS results of nanoWO_3|Lb$LTiO_2$|FeOOH|CoO_x-P_i after PEC water oxidation. Granulated particles are observable after PEC water oxidation. (a) and (a') shows the EDS spectrum analysed from the granulated particle (spectrum 1) and the granulated particle has a high atomic ratio of Co and Fe. On the other hand, (b) and (b') show no Co or Fe was detectable by EDS in the region without granulated particles (spectrum 2).

References

1. C.-Y. Lin, Y.-H. Lai, D. Mersch and E. Reisner, *Chem. Sci.*, 2012, **3**, 3482-3487.
2. B. Zhang, L. Wang, Y. Zhang, Y. Ding and Y. Bi, *Angew. Chem. Int. Ed.*, 2018, **57**, 2248-2252.
3. a) M. C. Biesinger, L. W. M. Lau, A. R. Gerson and R. S. C. Smart, *Appl. Surf. Sci.*, 2010, **257**, 887-898; b) U. Diebold; and T.E. Madey, *Surf. Sci. Spectra* 1998, **4**, 227.
4. M. Karbalaei Akbari, Z. Hai, Z. Wei, C. Detavernier, E. Solano, F. Verpoort and S. Zhuiykov, *ACS Appl. Mater. Interfaces*, 2018, **10**, 10304-10314.